Tectonophysics 749 (2018) 21–34

Contents lists available at ScienceDirect

Tectonophysics

journal homepage: www.elsevier.com/locate/tecto

New early Permian paleopoles from Sardinia confirm intra-Pangea mobility

V. Bachtadse[a,*], K. Aubele[a,b], G. Muttoni[c], A. Ronchi[d], U. Kirscher[e], D.V. Kent[f,g]

[a] Department of Earth and Environmental Sciences, Geophysics, Ludwig-Maximilians Universität, Theresienstr. 41, Munich 80333, Germany
[b] Munich School of Engineering (MSE), Technical University of Munich, Lichtenbergstr. 4a, Garching 85748, Germany
[c] Dipartimento di Scienze della Terra 'Ardito Desio', Università degli Studi di Milano, via Mangiagalli 34, Milan I-20133, Italy
[d] Dipartimento di Scienze della Terra, Università di Pavia, Via Ferrata 1, 27100 Pavia, Italy
[e] Earth Dynamics Research Group, ARC Centre of Excellence for Core to Crust Fluid Systems (CCFS) and The Institute for Geoscience Research (TIGeR), Department of Applied Geology, WASM, Curtin University, Perth 6845, Australia
[f] Rutgers University, Department of Earth and Planetary Sciences, Wright-Rieman Labs, 610 Taylor Road, Piscataway, NJ 08854-8066, USA
[g] Lamont-Doherty Earth Observatory, Columbia University, 61 Route 9W, Palisades, NY 10964-8000, USA

ARTICLE INFO

Keywords:
Paleomagnetism applied to tectonics
Permian
Sardinia
Paleogeography

ABSTRACT

We present new paleomagnetic results for the early and middle Permian (18 sites and 167 samples) from sedimentary and volcanic rocks from northern and central-southern Sardinia (Italy). Characteristic directions magnetization have been retrieved using stepwise thermal demagnetization techniques. The bedding corrected site mean directions for the northern and central-southern Sardinian basins show similar inclinations but differ significantly in declination indicating rotations of up to 55° between the two regions. No indication for inclination shallowing was observed. When corrected for the opening of the Ligurian Sea in the Cenozoic and the Bay of Biscay in the Cretaceous, the resulting paleopoles for northern Sardinia (Latitude 46.6°S, Longitude 46.7°W) and southern Sardinia (Latitude 42.8°S, Longitude 35.0°E), transferred into European coordinates are displaced from the coeval reference poles for stable Europe by ~30° clockwise and ~45° counterclockwise, respectively, with a rotation pole located close to the sampling region. Statistical parameters for the inclination-only mean for the 18 sites improve after applying the appropriate tilt corrections, suggesting that the magnetization was acquired before tectonic tilt and therefore allows to date the observed rotations to predate a mid Permian(?) folding event. These new results are in agreement with paleomagnetic data from the Sardinian dyke provinces and support earlier interpretations that the differences in general strike observed there are a secondary feature. Combining the data presented here with published data for the Corso-Sardinian block and the greater Mediterranean realm, we argue that the differential block rotations identified in Permian sediments and volcanic rocks reflect post-Variscan intra-Pangea mobility localized along a wide zone of deformation.

1. Introduction

Since the landmark papers of Irving (1967), Morel et al. (1981), and Morel and Irving (1978, 1981) a vivid debate on the validity of at least two Pangea configurations was sparked, which is still ongoing (Domeier et al., 2012, and references therein). Irving (1967, 1977) recognized that reconstructing Pangea in a Wegenerian (Pangea A) configuration for the latest Carboniferous-early Permian results in a significant overlap of both continents on the order of 1000 km. This dilemma was resolved by sliding Gondwana along lines of latitude some 3000 km to the east relative to Laurasia, thus positioning northwest Africa directly opposite the Donetsk basin in Ukraine (Morel and Irving, 1981, Fig. 1). The resulting Pangea B configuration resolves paleogeographically the problem of continental overlap, but assumes the existence of a megashear zone of some 3000 km along which Gondwana had to move to the west relative to Laurasia prior to the opening of the Atlantic, which started from a classical Pangea A configuration in the early Jurassic (Manspeizer, 1988, and references therein).

This westward translation could have occurred along a right lateral shear zone connecting the Urals and the Appalachians as originally proposed by Van Hilten (1964) as the "Tethys Twist" but which was erroneously attributed to the Mesozoic and subsequently revived by Arthaud and Matte (1977).

According to the most recent views based on critical reappraisals of paleomagnetic data, Pangea B existed in the late Carboniferous-early Permian as a consequence of Variscan convergence and coalescence between Gondwana and Laurasia, and then evolved into a Wegenerian Pangea A configuration by the late Permian (Muttoni et al., 2003, 2009;

* Corresponding author.
E-mail address: Valerian@lmu.de (V. Bachtadse).

https://doi.org/10.1016/j.tecto.2018.10.012
Received 2 July 2018; Received in revised form 29 September 2018; Accepted 7 October 2018
Available online 15 October 2018
0040-1951/

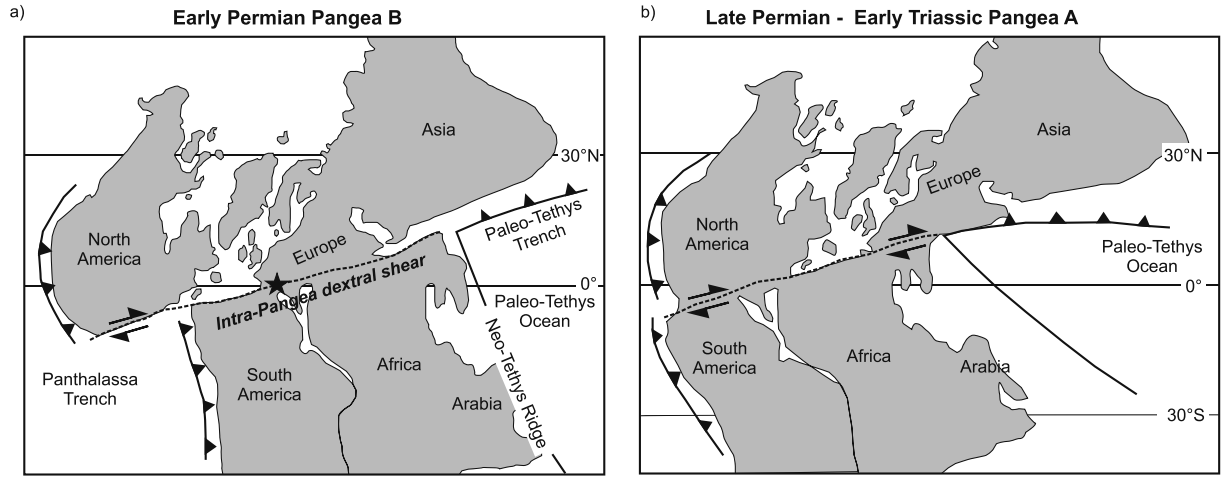

Fig. 1. Pangea B configuration after Irving (1977) in the early Permian (a). Star: approximate location of the study area. Wegenerian Pangea A configuration in the late Permian to early Triassic (b).
Source: Modified after Muttoni et al. (2009).

Angiolini et al., 2007; Gallo et al., 2017). In this scenario, the Pangea B to A transformation occurred within the (middle) Permian after the cooling of the Variscan basement and did not continue into the late Permian, Triassic as originally proposed by Irving (1977). In particular Muttoni et al. (2009) reconstructed an internally consistent global plate circuit during the opening of the Neo-Tethys ocean and the northward drift of Cimmerian terranes during the Permian.

Even though the concept of Pangea B has received ample supporting evidence from paleoclimatological (Fluteau et al., 2001), paleontological (Vai, 2003) as well as geochemical data (Becker et al., 2005), the strongest opposition arises from within the paleomagnetic community itself (see review by Domeier et al., 2012) and the different ways paleomagnetic poles from Gondwana and Laurasia are selected and used.

Thus the final outcome of the Pangea A versus B debate hinges, at least to some extent, on answering the question whether the existence of a large-scale intra Pangean transform fault zone (or diffuse plate boundary) can be demonstrated which is required to transfer Pangea from a B type into an A type configuration and which is most likely to run along the Permian paleoequator (Arthaud and Matte, 1977), in today's Mediterranean realm.

Transform fault activity causes differential vertical axis rotations of tectonic blocks caught within a wider fault zone (McKenzie and Jackson, 1983; Nicholson et al., 1986). These rotations can be identified and quantified by the analysis of paleomagnetic declinations. In combination with robust geochronological and stratigraphical control, paleomagnetism, therefore, allows substantial insights into the spatial and temporal (paleo-)evolution of (transform) fault activity in a given area.

If the intra Pangean shear zone model is valid, significant rotations of crustal blocks caught within the shear zone when it was most active are to be expected and can be mapped using paleomagnetic directional data.

To extend the existing set of Permian paleomagnetic data from Sardinia (REF), a detailed study of well dated intercalated sedimentary and volcanic sequences (Fig. 2) covering early Cisuralian to Guadalupian (early to middle Permian) is presented here. Fig. 3 shows a stratigraphic record of the sampled formations, which are described in detail in the following section.

2. Geological setting and stratigraphy

During latest Carboniferous to early Permian time interval strike-slip tectonic activity caused tilting and subsidence of basement blocks, triggering the formation of numerous pull-apart basins in Sardinia and elsewhere in western Paleoeurope (e.g., Cassinis et al., 1995; Broutin et al., 1994; Cassinis et al., 2000; Virgili et al., 2006; Cassinis et al., 2012; Gretter et al., 2015) and the deposition of thick piles of fluvial-lacustrine sediments. In Sardinia (Fig. 2) as in large parts of the Western Peri-Tethys, the post Variscan continental record can be broadly subdivided into three distinct tectono-sedimentary sequences (Fig. 3) or tectono-sedimentary cycles (*sensu* Virgili et al., 2006; Cassinis et al., 2012; Gretter et al., 2015). The time interval of interest is shown in Fig. 3. Hereafter, we describe the different areas of the island where Carboniferous-Permian to middle Triassic continental deposits crop out, starting from the northwest (NW) where all the sequences are represented and moving to the southwest (SW) where sequence I and probably II are present and lastly to the central southeast (SE) and northeast (NE) parts where only members of sequence I are present. We also note and will underline the close similarities between the Permo-Carboniferous basins of Sardinia and the Toulon-Cuers basin of southern France which has been the subject of a paleomagnetic study earlier (Aubele et al., 2012) and which can be correlated based on lithology, facies and chronostratigraphy.

2.1. Northwestern Sardinia

2.1.1. Lu Caparoni/Cala Viola Basin (Nurra)

The Nurra region (northwestern Sardinia, Fig. 2 represents the only part of Sardinia where the three Permian and Triassic clastic sequences are clearly exposed (Gasperi and Gelmini, 1980; Cassinis et al., 2003b; Ronchi et al., 2008; Baucon et al., 2014). From base to top a basal conglomerate overlain by a ~15 m thick alluvial to lacustrin succession composed of dark shales, sandstone layers and conglomerate bodies, Punta Lu Caparoni Formation (PLC, Gasperi and Gelmini, 1980; Cassinis et al., 2003b). On top of the PLC about 30 m of volcanoclastic acidic deposits (rhyolitic ignimbrites and tuffs; V1 in Fig. 3) are present. These volcanic rocks were recently dated as being 297 ± 1.8 Ma (U/Pb, Gaggero et al., 2017) and this age is in accordance with the macrofloral association found in this unit and which is indicative for the basal Cisuralian. Based on close lithological analogies, the PLC is assumed to be coeval with the Les Pellegrins Fm. in the Toulon-Cuers Basin (Cassinis et al., 2003b; Durand, 2006, 2008, and references therein). The PLC and volcanics V1 represent Sequence I; a moderate angular unconformity above PLC marks the boundary with the overlying Sequence II.

Sequence II starts with ~50 m of channelized conglomerates and sparse sandstones typical for braided alluvial environments (namely Pedru Siligu Formation in Sardinia (Fig. 3 and Transy Formation in souther France). After volcanic activity (V2 in Fig. 3; Casa Satta), dated as 288 ± 2.4 Ma (Gaggero et al., 2017) the area was characterized by

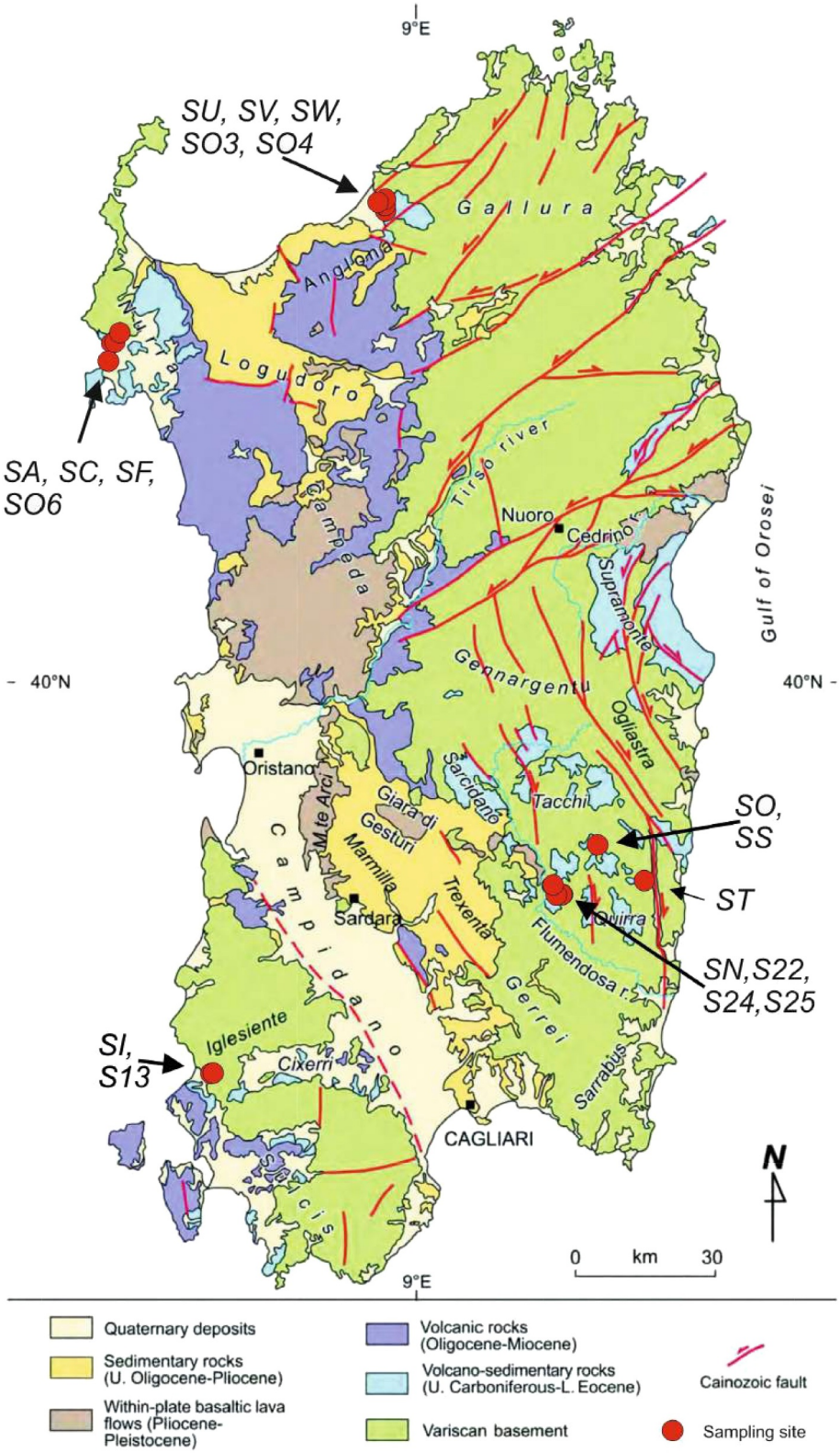

Fig. 2. Geological sketch map of the Upper Carboniferous-Permian sedimentary and volcanic sections in Sardinia. Red circles mark sampling locations. Source: Geological map taken from Carmignani et al. (2016).

the deposition of the Porto Ferro Formation consisting of at least 200 m of fossil-barren fluvial red beds. In the Provençal succession the Porto Ferro Fm. finds its correspondence with Les Salettes Fm. which yields at the top a lacustrine limestone (Bau Rouge limestone member), containing a latest early Permian, macro- and microflora (Durand, 2008). Above an angular unconformity follow ~400 m of stratified green to reddish sandstones and siltstones deposited in a meandering river system (Cala del Vino Formation). The Cala del Vino Formation can be correlated with the Provencal Saint-Mandrier Formation (Cassinis et al., 2003a; Durand, 2006, 2008) showing very similar lithofacies and

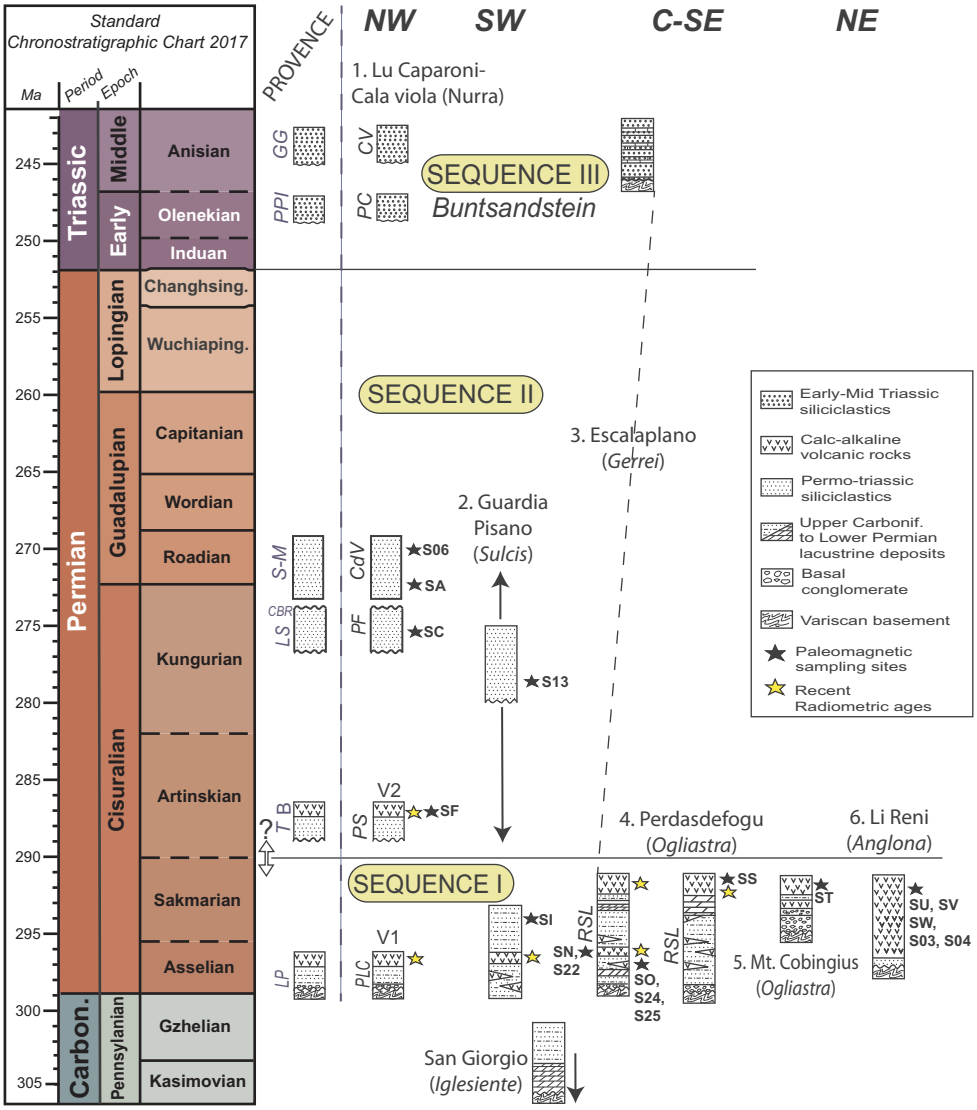

Fig. 3. Stratigraphy and ages of the sampled formations. PLC: Punta Lu Caparoni; PS: Pedru Siligu Formation; PF: Porto Ferro Formation; CdV: Cala del Vino Formation; CP: Porticciolo Conglomerate; CV: Cala Viola Formation; RSL: Rio su Luda Formation. Stars indicate the stratigraphic position of the sampled horizons.

fluvial architecture and rich in vertebrate fossils, which permitted to ascribe it to the early middle Permian.

In conclusion, Sequence I can be correlated with the basal Cisuralian, the lower part of Sequence II (Pedru Siligu and Porto Ferro formations to the early and late Cisuralian (early Permian) and the upper part of Sequence II (Cala del Vino Formation) to the latest Cisuralian-early Guadelupian (Roadian) based on new vertebrate finds (Ronchi et al., 2011).

The lowermost part of Sequence III (Porticciolo Conglomerate) rest unconformably on top of the Cala del Vino Formation, and starts with a few meters of quartz conglomerate, including wind-worn clasts and arenitic intercalations (Porticciolo Conglomerate). These deposits clearly testify to an arid environment, as recognized in many other parts of Europe during Olenekian times (late early Triassic) (Bourquin, 2007; Bourquin et al., 2011). Medium-to-fine grained red sandstones and siltstones, typical for floodplain deposits, characterize the overlying Cala Viola sandstones, indicating a sudden change from arid to semi-arid climatic conditions. The corresponding formations in the Toulon-Cuers basins are the Poudingue de Port-Issol and the Grés de Gonfaron (Cassinis et al., 2003a; Durand, 2006, 2008).

2.2. Southwestern Sardinia

2.2.1. Guardia Pisano (Sulcis)

According to some authors (Barca and Costamagna, 2006), the 120 m thick succession that is exposed in the Guardia Pisano Basin can be sub-divided into three informal lithostratigraphic units (the lower, middle and upper), where the latter two units seem to overlie the lower unit unconformably. On the basis of regional correlations, Ronchi et al. (2008) proposed later a subdivision of the section into four lithofacies (A to D) ranging in age from the early Cisuralian (facies A to C) to post-Autunian (late early Permian to middle Permian; facies D).

The basal deposits (A and B) are composed of grey-black sandy shales which were deposited in a fluvial-lacustrine to palustrine environment. For this unit of the Guardia Pisano sequence, an early Asselian age is indicated by a rich sporomorph record (Pittau et al., 2002) and in lithofacies B by a rich vertebrate fauna (Fischer et al., 2010). Unit B contains medium- to coarse-grained pyroclastic deposits and rhyolitic lava flows, which were radiometrically dated to 297 ± 5 Ma using SHRIMP and lead-zircon evaporation (Cocherie cited in Pittau et al., 2002). Unit C follows with about 45 m of barren medium–fine-grained reddish sandstones and micaceous siltstones with interstratified conglomerate layers and dark shale lenses. The upper unit

(D) is composed of grey to red sandstones and thin pelites deposited on an alluvial plain under warmer and humid conditions (Ronchi et al., 2008), due to a lack of fossil content, only a post-Asselian age can be constrained. Stratigraphical correlation with the deposits of Nurra (Pedru Siligu, Porto Ferro and Cala del Vino formations) is, for the time being, premature.

2.3. Central-Southeastern Sardinia

2.3.1. Escalaplano Basin (Gerrei)

In the Escalaplano Basin (Fig. 2) magmatic products clearly dominate over the strictly sedimentary units. The volcano-sedimentary succession can be subdivided into a lower and upper part (Pecorini, 1974; Cassinis et al., 2000; Ronchi et al., 2008). In general, both sequences start with coarse-grained sedimentary rocks followed by reworked volcaniclastic deposits and thus and ends respectively with a rhyolitic ignimbrite and with andesite lava flows. The ignimbrite capping the lower sequence yielded an age 302 Ma (U/Pb135 zircon data (Gaggero et al., 2017)), whereas the andesite lava flow was dated as being 294.6 ± 2.9 Ma in age based on single zircon U/Pb data (Gaggero et al., 2017). The whole Escalaplano succession (Sequence I and II) can be subdivided into nine lithostratigraphic units, seemingly separated by paraconformities as described in detail by Ronchi et al. (2008). Sequence I can in turn be subdivided into nine lithostratigraphic units, seemingly separated by paraconformities as described in detail by Ronchi et al. (2008). Up to date, on the basis of scarce (bio-)stratigraphical data and correlation with coeval successions from Sardinia (Sinisi et al., 2014) the Escalaplano deposits have been assigned a Cisuralian age (Ronchi et al., 2008).

2.3.2. Perdasdefogu Basin (Ogliastra)

The largest of the Permian sedimentary basins in south-eastern Sardinia hosts a Lower Permian volcano-sedimentary succession, nonconformably overlying the lower Paleozoic metamorphic basement and, in turn, unconformably covered by the middle to upper Jurassic coarse-grained quartz conglomerates and/or dolostones (Genna Selole and Dorgali formations). The basin fill is strongly influenced by contemporaneous volcanism, represented by calc-alkaline extrusives and dykes (Cassinis et al., 2000). The sedimentary and volcanic succession of the Perdasdefogu Basin has a total average thickness of 250 m. In this study, the dacites at the top of Riu Su Luda Formation (~30 m), 294.8 ± 3.5 Ma (U/Pb zircon, Gaggero et al., 2017) were sampled. For a detailed lithological description, the reader is referred to Ronchi et al. (2008). Based on studies by Ronchi et al. (1998, 2008), Cassinis et al. (2000), Cassinis and Ronchi (1997), and Galtier et al. (2011), significant similarities in the paleofloristic record exist between the Perdasdefogu succession and the sedimentary sequence in NW Sardinia (Nurra, Lu Caparoni Formation) The age of the Riu su Luda Formation can be paleontologically constrained by the co-occurrence of three amphibian species which can also be found in the Upper Goldlauter Formation in Thuringian Forest Basin, Germany (Werneburg et al., 2007).

2.3.3. Mt Cobingius

The Permian sedimentary succession at Monte Cobingius in eastern Sardinia, outcropping a few kilometers to the east of the main Perdasdefogu Basin, is mainly composed of Sequence I units: ~20 m of whitish conglomerates and sandstones of fluvial origin unconformably overlying the Variscan basemen. It is in turn covered by about 30 m of andesite breccias and lavas. A more detailed description of the sequence can be found in Ronchi et al. (2008).

2.4. Northeastern Sardinia

2.4.1. Li Reni (Anglona)

In the Coghinas Valley (Li Reni-Azzagulta area) of Anglona in NE Sardinia (Fig. 2) the Permian volcano-sedimentary sequence mainly attributed to Sequence I (Fig. 3) is exposed and represented by very scattered sedimentary deposits dominated by large volcanic effusive bodies (Traversa, 1979). Radiometric ages, obtained for Paleozoic sandstones at the base of the sequence and for the overlying ignimbrites (Rb/Sr on mineral separates, Muscovite and Biotite: 288 ± 3 and 286 ± 3 Ma, Del Moro et al., 1996) indicate an early-middle Artinskian (early Permian) age (Ronchi et al., 2008).

3. Field and laboratory methods

All samples were taken using a gasoline-powered, water-cooled drill and oriented using a standard magnetic compass. Subsequently, samples were cut into standard 11 cc cylindrical specimens. All samples were studied in the paleomagnetic laboratory of the University of Munich. The specimens were thermally demagnetized using a Schoenstedt furnace with increments of 30 °C up to maximum temperatures of 700 °C. Temperature steps were variably adjusted to sample behaviour during the demagnetization process and were decreased to 5 to 10 °C intervals approaching the unblocking temperature of the respective sample. After each heating step, the natural remanent magnetization was measured with a 2G Enterprises cryogenic SQUID (Superconducting QUantum Interference Device) magnetometer located in a magnetically shielded room. Demagnetization results were plotted on orthogonal projection diagrams (Zijderveld, 1967) and analyzed using the least square method (Kirschvink, 1980) on linear portions of the demagnetization paths defined by at least four consecutive demagnetization steps (Fig. 4). Linear fits were anchored to the origin of the demagnetization axes where appropriate. Data analysis was performed using the paleomagnetic software of Bachtadse (1994). Site mean directions are given in Table 1 and the resulting paleopole positions together with published data for the region are listed in Table 2. The paleomagnetic poles for Sardinia were transferred into European coordinates using the rotation parameters of Gong et al. (2008) to accommodate the opening of the Bay of Biscay and of Gattacceca et al. (2007) for the opening of the Ligurian sea. The resulting combined rotation pole has the coordinates $lat = 41.93°$, $long = 4.61°$ with an angle of $-79.8°$ (clockwise).

In addition to paleomagnetic analyses, rock-magnetic properties were determined using a Variable Field Translation Balance (Krása and Fabian, 2007, Fig. 5). Rock magnetic analyses include hysteresis measurements, isothermal remanent magnetization (IRM) acquisition in fields up to 700 mT, backfield magnetization defining the coercivity of remanence, and in-field heating (up to 700 °C) and cooling cycles (hereafter referred to as thermomagnetic measurements) in order to estimate the Curie temperatures of the magnetic minerals (Moskowitz, 1981), as well as to identify possible mineralogical transformations during heating. Analysis of the rock magnetic parameters was carried out using the software by Leonhardt and Soffel (2006).

4. Results

4.1. NRM demagnetization behaviour/magnetic mineralogy

4.1.1. Northern Sardinia (Gallura and Nurra)

Fig. 4 shows five representative orthogonal projection diagrams from sites in northern Sardinia (S03-7A, S04-5A from Gallura and S06-7A, SA-6A and SC-14B from Nurra). The samples from Gallura show comparable demagnetization behaviour with essentially two directional components. The low temperature (LT) component in samples S03-7A and S03-4A is removed by heating up to 250 °C. It has roughly the same direction of the present day magnetic field for Sardinia which is $D = 359°$, $I = 55°$ (calculated from the 2014 version of the international geomagnetic reference field model IGRF-12: http://www.ngdc.noaa.gov/IAGA/vmod/igrf.html, 01/12/2018). The high temperature (HT) component shows a clear trend towards the origin of the orthogonal

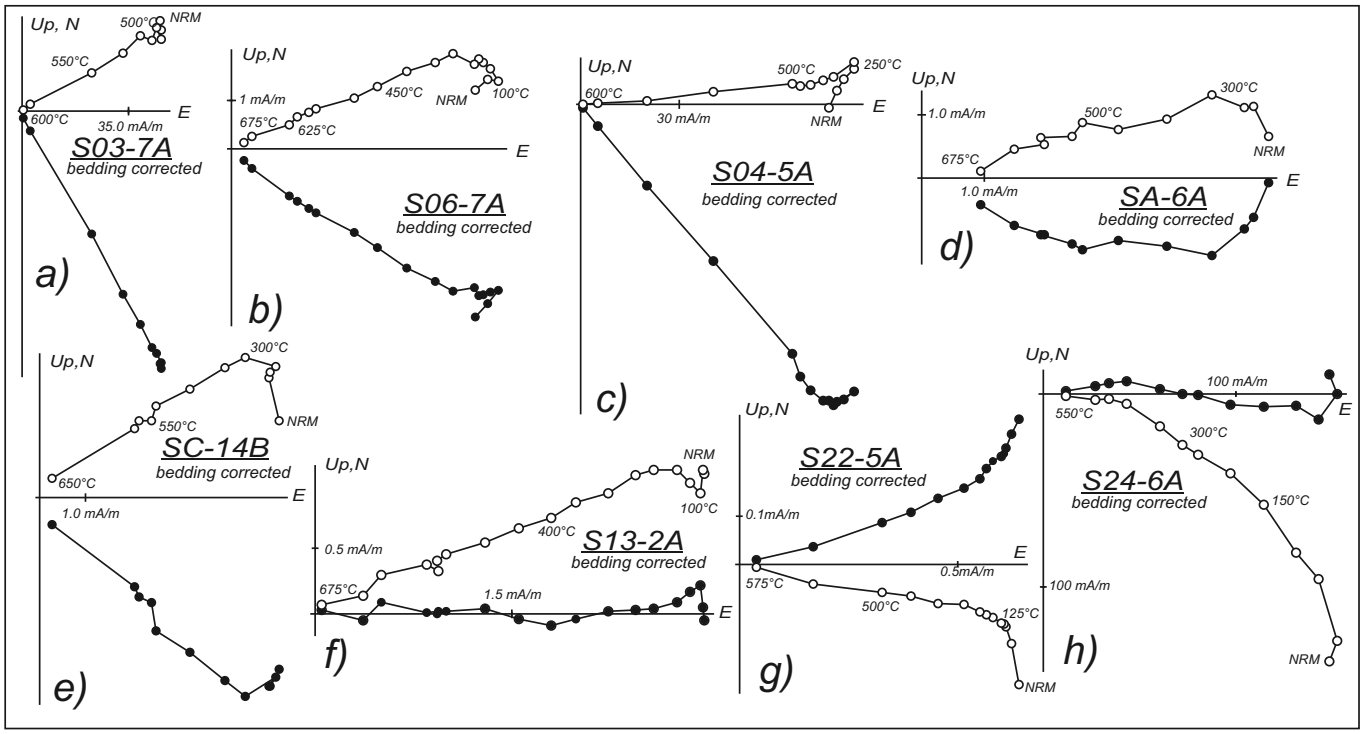

Fig. 4. Results of thermal demagnetization experiments plotted as orthogonal vector diagrams (Zijderveld, 1967) in geographic coordinates. Solid and open dots represent vector endpoints projected onto the horizontal and vertical planes, respectively. a–e are representative data from the northern part of Sardinia, f–h from the southern-central part. c, g, and h are representative for the volcanic rocks studied, whereas a, b, d, e and f are for the reddish sediments.

projection with magnetization intensity gradually decreasing during stepwise heating up to 600 °C. Sample S04-5A (Fig. 4c) also shows two directional components during thermal demagnetization. LT is removed by heating up to 250 °C, whereas HT shows a clear trend towards the origin of the diagram with a gradual decrease in magnetization intensity up to 625 °C. The samples from the Nurra region show more variable demagnetization behaviours with more than one directional components. In samples S06-7A and SC-14B (Fig. 4b and e), no clear low temperature directional component can be defined. However, from 300 °C onward, a single component trending towards the origin of the diagram can be clearly defined in both samples. Magnetization intensity gradually decreases during stepwise heating up to 650–675 °C. Sample SA-6A (Fig. 4d) shows three directional components. The first component is removed at 300 °C, the second one at 500 °C. Up to 675 °C, the third component trends towards the origin of the demagnetization diagram.

Fig. 5 shows representative results from rock-magnetic experiments. The results from sample S06-8 give a clear indication of magnetite as the main carrier of magnetization (Fig. 5a). The Curie temperature of ~580 °C and the coercivity of remanence (obtained from backfield curve measurements) of ~30 mT support this interpretation. The results for sample SC-4 (Fig. 5 b) also from the northwestern sampling area, on the other hand, strongly suggest the presence of two coercivity fractions. The wasp-waisted shape of the hysteresis loop as well as the two-step decrease in the thermomagnetic heating curve at ~580 °C and ~650 °C, respectively, indicate magnetite and haematite as main magnetic carriers. The coercivity of remanence of ~140 mT is the weighted result of the contributing high- and low-coercivity fractions. Values for magnetite typically lie in the range of a few tens of mT, while haematite is typified by values of a few hundreds of millitesla (Dunlop and Argyle, 1997). The obtained value of ~140 mT is therefore likely to be the result of a combination of both carriers. Both samples do also show a decrease of intensity at ~100 °C, which might be related to the presence of minor amounts of goethite. This is in agreement with the lack of non-closure of the hysteresis loops.

4.1.2. Central-southern Sardinia (Gerrei and Iglesiente/Sulcis)

Fig. 4 displays two representative demagnetization diagrams from samples from the Gerrei sites (Escalaplano: S22-5A and S24-6A). Both samples show two overlapping directional components. The low temperature component, pointing roughly towards the direction of the present day magnetic field for Sardinia (again calculated from the IGRF-12 model), is removed at ~100 °C. In both samples, the second component shows a clear trend towards the origin of the demagnetization diagram, with gradually decreasing magnetization intensity up to 550–575 °C. Directional data from site S13 (Sulcis) are presented in Fig. 4. A low stability secondary component is removed at ~100 °C. A vector end point trajectory trending towards the origin of the orthogonal projection can be defined for the demagnetization steps from 200 to 700 °C. Rock-magnetic results from the samples from central-southern Sardinia are displayed in Fig. 5c–e. The samples from the Gerrei area (Fig. 5c and d) provide clear evidence of magnetite as the main magnetic phase. This is especially evident in sample S24-2, where the rather low coercivity of remanence of ~45 mT and the typical convex decrease in magnetization intensity displayed by the heating portion of the thermomagnetic curve, culminating in a Curie temperature of 577 °C, provide substantial evidence for this observation. The picture is a little less clear in sample S25-6. We speculate on a more pronounced presence of goethite in accordance with the initial decrease in magnetization at ~100 °C, as displayed in the heating portion of the thermomagnetic curve. The second decrease in magnetization intensity at 587 °C, however, is indicative of magnetite. Fig. 5e shows data from site S13 from the Sulcis area. The strong paramagnetic content and high coercive fraction are clearly visible in the hysteresis curve. The sudden drop in intensity at about 660 °C provides clear evidence for the existence of haematite as primary magnetic phase. Some minor amounts of goethite visible in the thermomagnetic curve might also add to the high coercivity fraction.

4.2. Paleomagnetic mean directions

A low temperature component (up to 300 °C) was identified in almost all samples with the exception for those collected in the Iglesiente/Sulcis area, clustering around the present day field direction calculated for a nominal point at 40°N/9°E in Sardinia using the IGRF-12 model (Fig. 6).

4.3. Northern Sardinia (Gallura and Nurra)

A total of 83 samples from 9 sites from northern Sardinia were included in the analysis (Fig. 2 and Table 1). In northwest Sardinia, samples were taken from the Pedru Siligu, Porto Ferro and Cala del Vino Formations (Fig. 3). In addition, we sampled the Permian ignimbrites in Gallura, which were previously studied by, among others, Zijderveld et al. (1970) and Westphal et al. (1976). As the ignimbritic formation lies approximately horizontal and the local structural setting appears undeformed, no tectonic correction was applied here. The site mean directions in *in situ* and in bedding corrected coordinates are shown in Fig. 7a, b. The Permian site mean direction from northern Sardinia yields a bedding corrected regional mean direction for the area of $Dec = 135.0^\circ$, $Inc = -14.6^\circ$ (N = 9, $\alpha_{95} = 14.0^\circ$, $k = 14.4$). This is in substantial agreement with the previous results for Gallura of Zijderveld et al. (1970, $Dec = 142.0^\circ$, $Inc = -2.0^\circ$, N = 6, $\alpha_{95} = 12.0^\circ$, $k = 34$) and of Westphal et al. (1976, $Dec = 145.0^\circ$, $Inc = 0.0^\circ$, N = 4, $\alpha_{95} = 27.0^\circ$, $k = 1$).

4.4. Southern Sardinia (Iglesiente/Sulcis and Gerrei/Ogliastra)

A total of 84 samples from 9 sites ranging in age from early to middle Permian from central-southern Sardinia were included in the analysis (Figs. 3, 2 and Table 1). 22 samples from two sites from the Iglesiente/Sulcis and 62 samples from 7 sites from the Gerrei/Ogliastra region yield a bedding corrected mean direction for central-southern Sardinia of $Dec = 81.1^\circ$, $Inc = 7.7^\circ$ (N = 9, $alpha_{95} = 9.7^\circ$, $k = 28.9$, Fig. 7c, d). This supports previous results for central-eastern Sardinia from our study on Paleozoic dykes on Sardinia of $Dec = 91.9^\circ$, $Inc = -4.8^\circ$ (N = 6, $\alpha_{95} = 13.6^\circ$, k = 25.3 Aubele et al., 2014) and also with results from southeast Sardinia from Edel et al. (1981, $Dec = 85.0^\circ$, $Inc = -7.0^\circ$, N = 27, $\alpha_{95} = 5.5^\circ$, k = 27, Table 2).

5. Data interpretation

The site mean directions from this study show shallow (negative and positive) inclinations with declinations pointing either to the SE or E depending on their regional provenance (northern vs. central-southern Sardinia) differing by ~ 45° (Fig. 7). The inclination only regional fold test (McFadden and Reid, 1982) results in an increase of the Fisher (1953) precision parameter k from 19.5 to 33.9 and supports the interpretation of the magnetization being acquired prior to tilting. The resulting regional mean directions for northern and central-southern Sardinia as well as results from previously published studies of the Permian of Sardinia and Corsica are listed in Table 2 and shown in

Table 1
Paleomagnetic results.

Site					In situ				Bedding corrected			
Name	*n/N*	*Lithology*	*GLat* [°N]	*GLon* [°E]	*Dec* [°]	*Inc* [°]	*k*	α_{95} [°]	*D* [°]	*I* [°]	*k*	α_{95} [°]
Northern Sardinia (Gallura, Nurra)												
SA	9/13	Redbeds	N40.64	E8.19	115.6	−26.6	26.1	10.3	116.2	−20.3	26.1	10.3
SC	14/14	Red siltstone	N40.68	E8.20	87.9	−60.3	10.9	12.6	124.1	−39.9	11.7	12.2
S06	7/10	Redbeds	N40.68	E8.20	113.3	−16.5	10.3	19.7	114.3	−9.7	10.9	19.2
SF	9/15	Volcanics	N40.70	E8.22	129.6	−3.5	6.2	22.5	130.8	−14.1	6.3	22.4
SU	7/12	Ignimbrites	N40.94	E8.90	142.5	−8.0	40.5	9.6	142.5	−8.0	40.5	9.6
SV	21/23	Ignimbrites	N41.00	E8.90	137.7	−7.6	22.4	6.9	137.7	−7.6	22.4	6.9
SW	7/8	Ignimbrites	N40.95	E8.87	145.5	2.9	16.5	15.3	145.5	2.9	16.5	15.3
S03	5/13	Ignimbrites	N40.93	E8.89	150.4	−10.2	23.3	16.2	150.4	−10.2	23.3	16.2
S04	4/8	Ignimbrites	N40.94	E8.89	145.5	−4.1	72.2	10.9	145.5	−4.1	72.2	10.9
Site mean	9/9				132.8	−15.0	10.5	16.7	135.0	−14.6	14.4	14.0
Southern Sardinia (Iglesiente, Gerrei)												
SI	16/33	Redbeds	N39.25	E8.46	85.6	3.3	21.6	8.1	86.9	18.8	20.6	8.3
S13	6/10	Redbeds	N39.25	E8.45	78.9	−10.3	24.8	13.7	81.1	−8.4	25.7	13.5
SN	8/20	Ignimbrites	N39.62	E9.32	68.5	2.2	310.5	3.1	68.4	7.1	129.0	4.9
SO	9/14	Rhyolitic tuffs	N39.61	E9.35	92.2	15.3	9.2	17.9	96.4	20.1	9.2	17.9
SS	20/20	Dacite	N39.70	E9.43	82.9	−10.0	40.3	5.2	84.5	−4.3	40.3	5.2
ST	4/8	Andesite	N39.63	E9.55	81.2	12.2	61.4	11.8	76.4	27.3	61.4	11.8
S22	7/9	Ignimbrites	N39.62	E9.32	72.3	−8.9	17.9	14.7	73.5	−3.6	27.5	11.7
S24	8/8	Rhyolitic tuffs	N39.60	E9.34	86.0	0.3	16.3	14.1	82.8	2.9	13.7	15.5
S25	6/7	Rhyolitic tuffs	N39.60	E9.33	81.3	−9.0	47.5	9.8	82.9	−6.4	19.5	15.5
Site mean	9/9				81.0	−0.6	45.1	7.7	81.1	7.7	28.9	9.7
Inclinations only mean (Tauxe, 2010)												
	18/18					−11.7	19.5	7.0		−11.5	33.9	4.9

n/N: number of specimens used calculate the mean direction/number of specimens measured, GLat/GLon: Geographic latitude/longitude of sampling site; Dec and Inc: declination and inclination of site mean direction respectively; α_{95}: Circle of 95% confidence (Fisher, 1953).

Table 2
Permo-Triassic pole positions for Corsica-Sardinia from the literature and from the present study rotated to European coordinates.

Region	Label	Age	D	I	α_{95}	Pole position				REF
			[°]	[°]	[°]	Corso-Sardo c.		European c.		
						[°S]	[°E]	[°S]	[°E]	
Corsica	1	320–250	134.7	−11.3	6.8	36.3	70.4	46.5	−44.5	[1]
Sardinia	2	320–250	132.7	−1.6	7.3	31.2	68.4	43.6	−38.1	[1]
Nurra	3	296 ± 9	126.0	−1.0	–	26.6	73.9	46.6	−29.7	[2]
Nurra	4	Permian	110.0	−15.5	–	20.0	91.0	58.2	−9.2	[3]
Gallura	5	Permian	142.5	−2.0	11.5	38.0	59.0	38.8	−52.8	[3]
Gallura	6	Permian	145.0	0.0	27.0	37.0	58.0	37.0	−48.7	[4]
NE Sardinia	7	282 ± 4–268 ± 4	133.1	1.2	15.0	31.5	67.9	43.3	−38.7	[5]
N Sardinia	8	295–270	135.0	−14.6	14.0	38.0	71.4	47.6	−64.8	This study
Mean pole	A				8.7			46.1	−43	
SE Sardinia	9	300–280	85.0	−7.0	5.5	1.3	−75.6	51.0	33.6	[2]
E Sardinia	10	298 ± 5–289 ± 4	91.9	−4.8	13.6	3.0	100.1	52.7	24.0	[5]
SE Sardinia	11	298 ± 5–289 ± 4	80.0	−20.6	24.2	0.9	−66.0	54.9	48.2	[5]
S Sardinia	12	298–290	81.1	7.7	9.7	9.3	−78.3	42.8	35.0	This study
Mean pole	B				9.2			50.6	35.0	

Rotation parameters: Gattacceca et al. (2007) (rotation pole coordinates λ = 43.50°, φ = 9.50°, angle 45.00° cw) to close the Ligurian ocean and Gong et al. (2008) (rotation pole coordinates λ = 43.00°, φ = −2.00°, angle 35.00° cw) to account for the opening of the Bay of Biscay. All poles are projected to the southern hemisphere. Labels refer to the poles as plotted in Fig. 8. Also listed are the presumed magnetization ages (numbers in Ma), declination (D) and inclination (I) as taken from the original publication, the 95% confidence limit (α_{95}) (Fisher, 1953) on the calculated mean direction, the resulting pole positions (Corso-Sardo coord.) and the pole position correct for the opening for the Gulf of Lyon (European coord.) REF: References, [1]: Vigliotti et al. (1990); [2]: Edel et al. (1981); [3]: Zijderveld et al. (1970); [4]: Westphal et al. (1976); [5]: Aubele et al. (2014).

Fig. 8.

Site mean directions from the northern and central-southern parts of Sardinia for volcanic and sedimentary rocks group in the SE and E of the equal area projection of Fig. 7, respectively, differing by 52.5° in declination. Although, results from sedimentary rocks are somehow underrepresented in the current study, we do not, at first sight, observe any indication for inclination shallowing. In order to test this assumption further, we have calculated a regional mean declination (107°, after application of a 45° cut-off angle) based on the individual mean directions of the four sampling areas (Nurra, Gallura, Gerrei and Iglesiente). In a second step we have determined the angular difference (δD) between the overall mean declination and the mean declinations

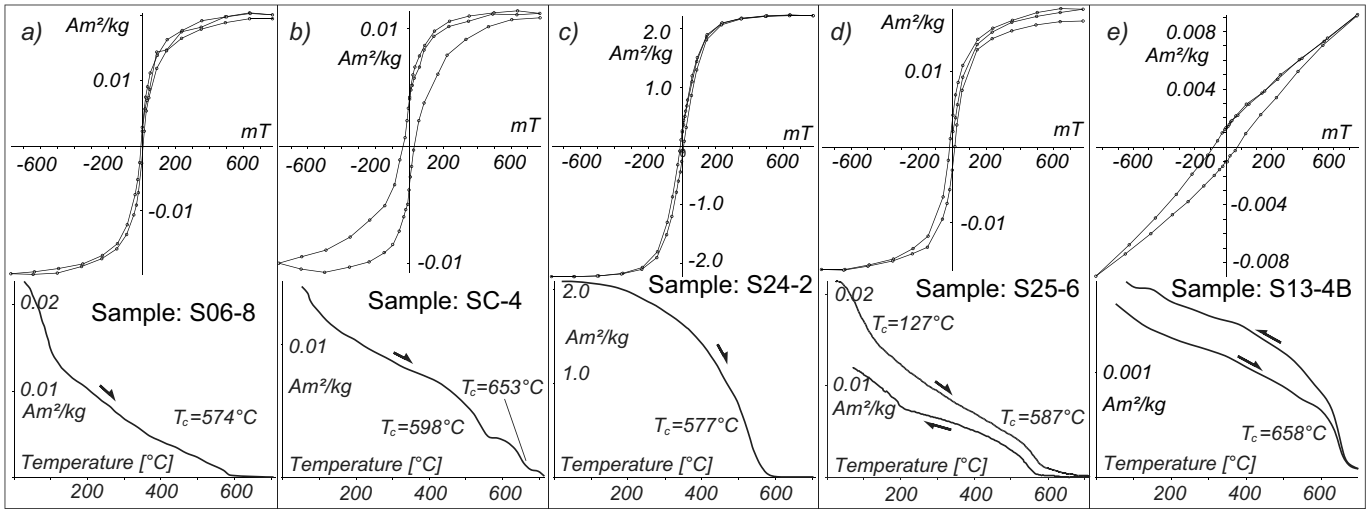

Fig. 5. Results of rock-magnetic experiments on representative samples. Hysteresis loops (top) and corresponding thermomagnetic curves (bottom). Intensities are given in Am^2/kg.

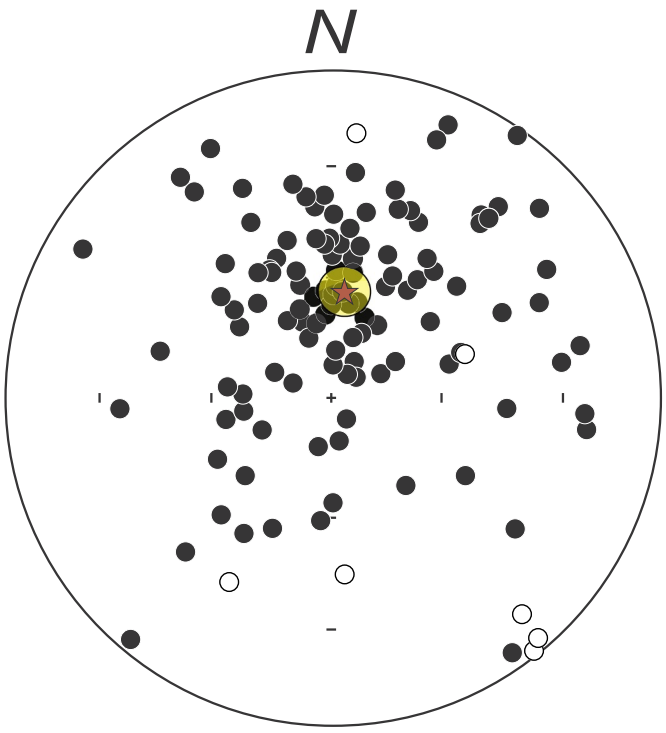

Fig. 6. Stereographic projections in bedding corrected coordinates of the low temperature magnetic component directions of samples from this study. Solid and open dots represent projections on the upper and lower hemispheres, respectively. LT component directions from Gerrei ($D = 359.6^{\circ}$, $I = 59.7^{\circ}$, $\alpha_{95} = 10.0^{\circ}$, $k = 3.8$), Nurra ($D = 11.3^{\circ}$, $I = 39.8^{\circ}$, $\alpha_{95} = 9.7^{\circ}$, $k = 4.6$), and Gallura ($D = 5.2^{\circ}$, $I = 57.8^{\circ}$, $\alpha_{95} = 7.2^{\circ}$, $k = 10.5$).

for each of the four sampling regions. In a final step, all individual directions of the characteristic remanent magnetization have been rotated applying δD (Nurra: − 17.6°, Gallura: − 35.5°, Gerrei: + 26.5° and Iglesiente + 26.5°) before applying the elongation inclination test (Tauxe and Kent, 2004) on the combined data set. Our procedure assumes that tectonic rotations affected declination values, but each within site scatter is due to secular variation. We point out that applying a 45° cut-off angle and a correction of tectonic rotation both might affect the elongation-inclination correction approach. However, there is significant within-site scatter that should reflect secular variation sufficiently. Also, the cut-off seems justified in removing only actual outliers (Fig. 9). Ultimately, this approach is definitely not a final judgment and a more detailed study would be necessary to solve this issue. After correction for the tectonic rotation, we can compare the individual directions from all the four areas. This results in a corrected inclination of − 7.0° (initial value of − 5.1°) with an uncertainty interval, which includes the uncorrected inclination value (Fig. 9). This is strong support of our assumption that magnetization in coeval sedimentary and in volcanic rocks have been acquired rather simultaneously and therefore the directions isolated in the sedimentary rocks are representative of the geomagnetic field during magnetization acquisition. This result also questions the validity of recently published apparent polar wander paths for the Permian, which use a single global correction for sedimentary inclination shallowing ($f = 0.6$, Domeier et al., 2012).

In order to compare our new and previously published paleomagnetic data for the Permian of the western Mediterranean, we have defined mean paleopoles for the late, mid and early Permian based on volcanic rocks listed in Table 1 of Torsvik et al. (2012) exclusively and calculated the resulting mean poles for early mid and late Permian times (Table 3). In a second step, the directional data obtained in this study were translated into paleopole positions and the latter corrected for the rotation of Spain (Gong et al., 2008) and the opening of the Ligurian Sea (Gattacceca et al., 2007) yielding two distinct clusters: Permian paleomagnetic (south) poles from northern Sardinia plot to the west of the Permian reference poles for Europe (Fig. 8)

The poles from this study as well as the published poles of similar

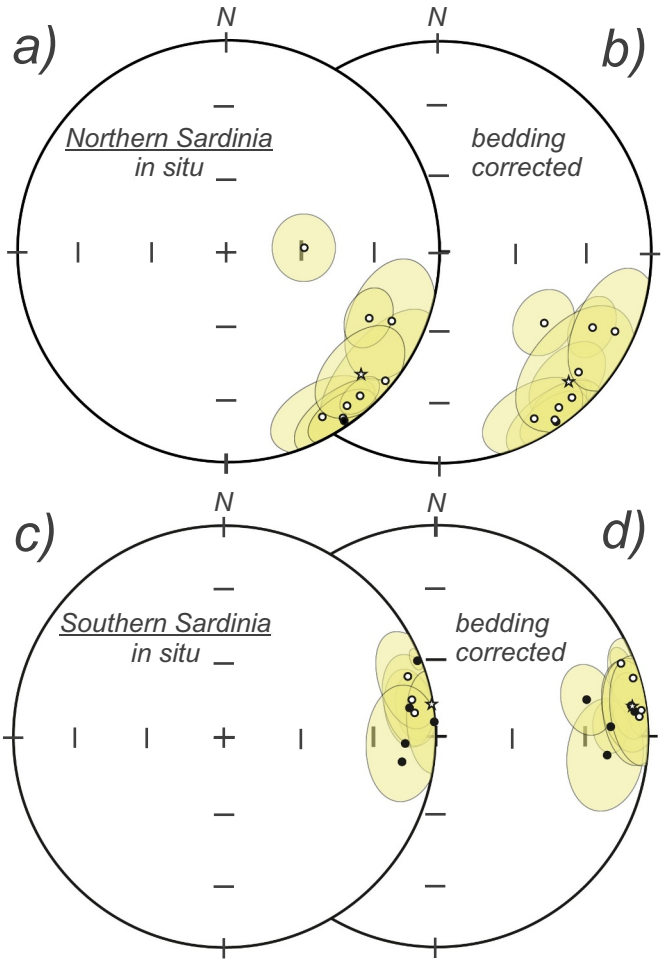

Fig. 7. Stereographic projections of site mean directions (circles) and overall mean direction (star) for northern Sardinia (a, b) and central-southern Sardinia (c, d). The directions are shown with their associated 95% confidence ellipses (Fisher, 1953) in in situ (a, c) and bedding corrected coordinates (b, d). Solid and open symbols represent projections on the upper and lower hemispheres, respectively.

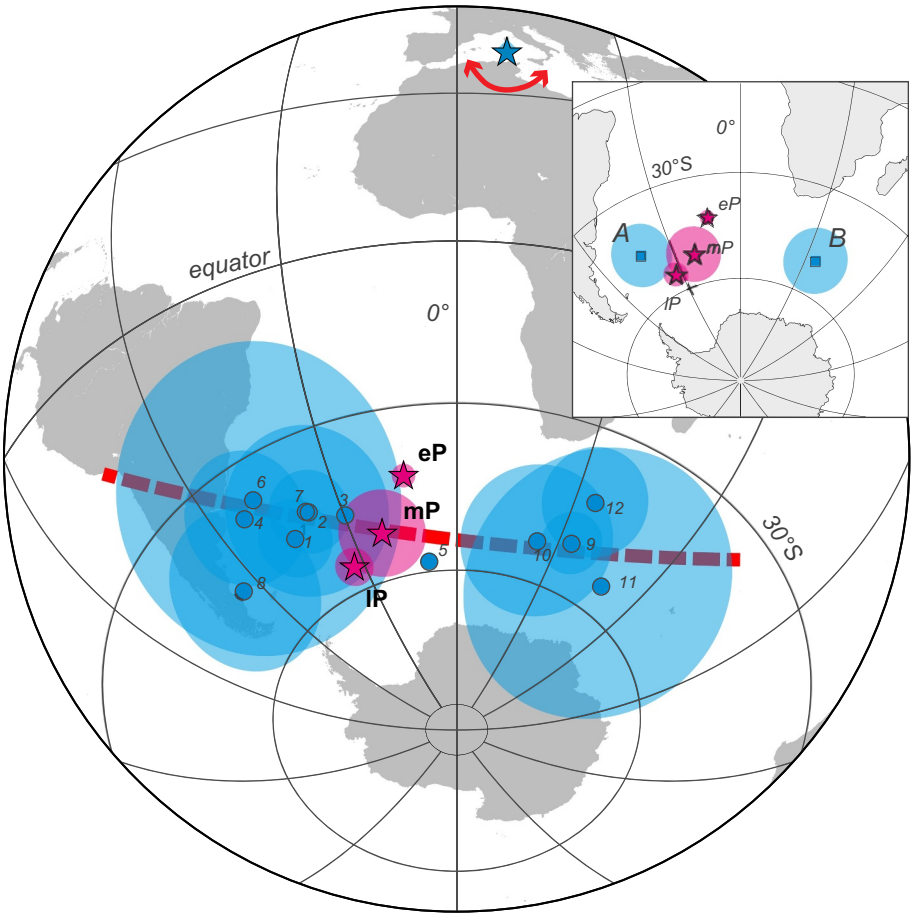

Fig. 8. Paleomagnetic poles from this study for northern (8) and southern Sardinia (12) in combination with other published poles for the Permian of the Sardinia -Corsica block (in blue). The reference paleopole positions for stable Europe (in red, see also Table 3) are plotted together with the 95% confidence ellipses (Fisher, 1953). eP: early Permian, mP: mid Permian, lP: late Permian. The labeling on the Sardinia-Corsica pole positions is according to Table 2. The resulting pole of rotation is marked by the blue star. The inset shows the resulting mean pole positions for northern Sardinia- Southern Corsica (A) and souther-central Sardinia (B). Red dotted line indicates small circle deviations around the sampling site.

age for the western Mediterranean are distributed along a small circle swath including the European reference poles for the early and mid Permian in broad agreement with the mean ages of the sampled rocks (Fig. 8). Fitting a small circle to the data results in a single Euler pole of rotation, which accounts for the differential block rotations observed; this Euler pole lies close to the study area at *lat* = 40°N, *long* = 9°E (Fig. 8) and suggests differential true vertical axis rotations between the central-southern and northern parts of Sardinia during the early Permian in agreement with earlier studies (Kirscher et al., 2011; Aubele et al., 2014).

In order to estimate the Permian rotations of northern and central-southern Sardinia relative to stable Europe, we restored those regions to European coordinates using the rotation procedure outlined above, obtaining a position for a nominal point at the centre of northern Sardinia of *lat* = 38.6°N, *long* = 4.2°E and for a nominal point at the centre of central-southern Sardinia of *lat* = 37.9°N, *long* = 2.8°E. These restored coordinates were then used to calculate the declinations and inclinations expected from paleomagnetic poles of this study in European coordinates. The resulting directions are: *Dec* = 211.9°, *Inc* = −14.6° for northern Sardinia and *Dec* = 156.9°, *Inc* = 8.3° for central-southern Sardinia. The expected directions for the different parts of Sardinia (restored to Europe) calculated from the mid Permian reference paleopole of Table 3 are *Dec* = 195.8°, *Inc* = −6.2° for northern and *Dec* = 194.9°, *Inc* = −4.2° for central-southern Sardinia, which implies differences in declinations of 18° for northern and 40.0° for central-southern Sardinia. Fig. 10 shows northern and central-southern Sardinia in its present outline (a) and restored to the early Permian paleogeography (b). In the restored configuration, the early Permian dykes show a much better alignment which is in agreement with what we observed before (Aubele et al., 2014).

6. Conclusion

In conclusion, the results of this study confirm previous results from various regions within Sardinia and obtained from different rock types. The paleomagnetic mean direction from central-southern Sardinia is virtually identical with the direction from the eastern dyke province from Sardinia (Aubele et al., 2014), which is an independent validation that the dykes were not tilted about horizontal axes. This is a confirmation for the suitability of dykes for paleomagnetic sampling, as long as a reference surface for tectonic correction can be reliably defined. With this study, we substantiate the observation of true vertical

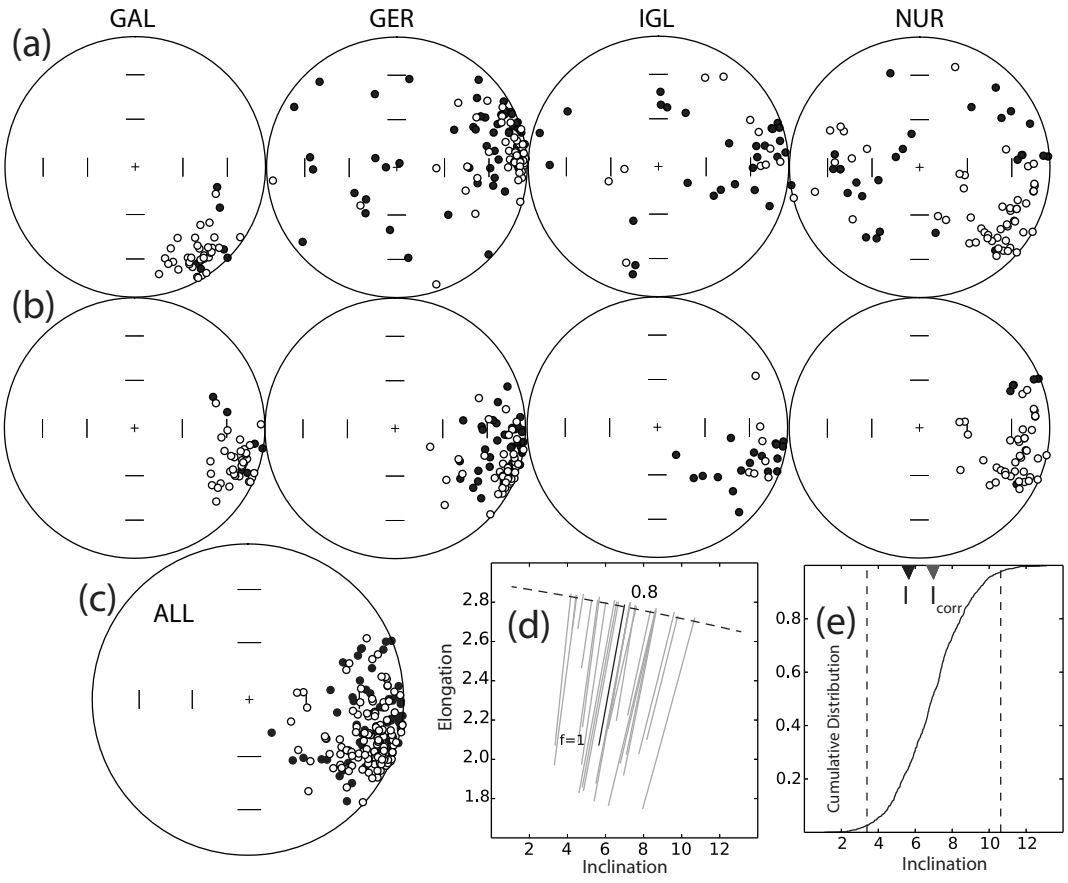

Fig. 9. Elongation/inclination (E/I) method of Tauxe and Kent (2004), for detection of potential inclination shallowing. (a) Stereographic projection of sample mean directions for individual areas (GAL-Gallura, GER-Gerrei, IGL-Iglesiente, NUR-Nurra). (b) Same as (a) after applying a 45° cut-off and rotating to a common mean declination of 107°. (c) Combined mean direction data. (d + e) Result of E/I method yielding an f value of 0.8 and a corrected inclination of 7° with an uncertainty interval between 3.4° and 10.6°.

Table 3
Permian reference poles for stable Europe.

Epoch	Lat. [°S]	Long. [°E]	N –	k –	A_{95} [°]
Late Permian	55.7	326.7	7	321.1	3.4
Mid-Permian	51.7	338.3	4	140.1	7.8
Early Permian	42.4	347.1	37	122	2.1

Reference poles for stable Europe based on data from volcanic rocks exclusively, taken from Torsvik et al. (2012). Age assignment after the Permian timescale (Shen and Henderson, 2014). Lat.: Latitude, Long.: Longitude, N: number of individual pole positions used, the Fisherian confidence parameters k and A_{95} (Fisher, 1953).

axis rotations (clockwise and counterclockwise) within a broad band of crustal segments in the western Mediterranean during early and middle Permian times. This observation testifies to general intra-Pangea mobility associated with large-scale shearing between Laurasia and Gondwana that must have occurred sometime after the middle Permian. In fact, we can define three crustal blocks within the study areas in the western Mediterranean as indicated in Fig. 11. The southern block 1 rotated counterclockwise with respect to stable Europe and the adjacent blocks after magnetization acquisition in the early Permian. The central block 2 on the other hand shows a slight clockwise rotation with respect to both, stable Europe and block 1 after magnetization of the sampled rocks in the early Permian. Early Permian results from the northern block 3 show a large clockwise rotation with respect to stable Europe as well as to blocks 1 and 2. We conclude in favor of a decreasing N-S gradient in rotation rates towards the south and away from the northern boundary of the large-scale transform fault zone (in late Paleozoic/early Mesozoic coordinates). The counterclockwise rotation of block 1 confirms the ball bearing model that was recently proposed (Aubele et al., 2012), which leads to clockwise and counterclockwise rotations of blocks of different aspect ratios caught within large-scale transform fault zones.

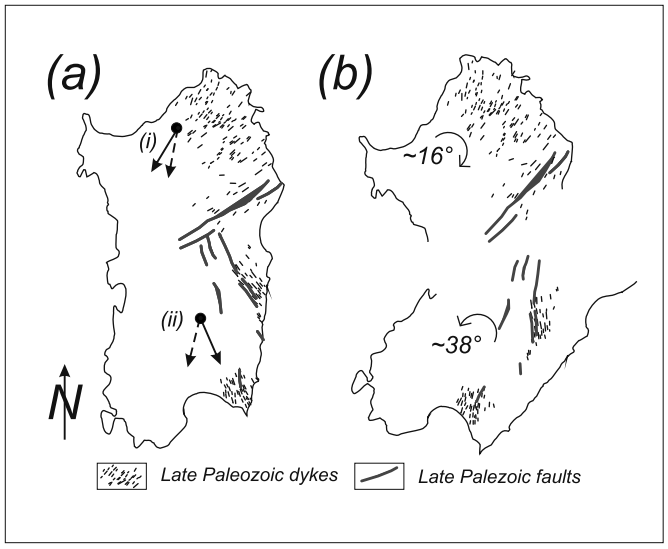

Fig. 10. (a) Sardinia in its present outline and orientation with the distribution of early Permian dyke provinces. Stippled: expected Permian declinations for (i) northern Sardinia and (ii) central-southern Sardinia calculated from the early Permian reference pole for stable Europe (Table 3). Solid: observed magnetic declinations of the early Permian samples of this study. All declinations are in European coordinates (e. g. corrected for the opening of the Bay of Biscay and of the Liguro-Provençal Basin). (b) Paleogeography of Sardinia restored based on the observed declinations; the arrows indicate the amount and sense of rotation since the magnetization was acquired.

We know from earlier studies (Advokaat, 2011; Kirscher et al., 2011; Aubele et al., 2012) that the western Mediterranean area - namely the Maures-Esterél Massif, the Toulon-Cuers Basin, Corsica and Sardinia - acted as a single tectonic block from at least 260 ± 10 Ma (late Permian) onward until the Cenozoic counterclockwise rotation of Corsica-Sardinia away from the European mainland. However, a more precise determination of the time of rotation remains elusive. Including the statistically poorly defined paleomagnetic pole from Zijderveld et al. (1970) for the Nurra region (Sardinia) in the database (Table 2), the upper age constraint of the observed rotations can be tentatively put in the uppermost Permian (~260 Ma). This upper time limit for transform fault activity between Laurasia and Gondwana is perfectly reconcilable with paleogeographic reconstructions based on paleomagnetic data for the late Permian, which allow a Pangea A configuration (Muttoni et al., 2003; Torsvik et al., 2012).

Acknowledgements

We thank editor Rob Govers for handling the manuscript. Very constructive comments by Mat Domeier and one anonymous reviewer significantly improved the quality of this paper. This project has been funded by the German Research Foundation (DFG) Grants BA 1210/8-1 and BA 1210/20-1. Special thanks go to Barbara Emmer (now Huber), Elmar Moser and Matthias Hackl for assistance in the field during the various field campaigns.

Unlimited access to the raw data will be provided by the authors upon request.

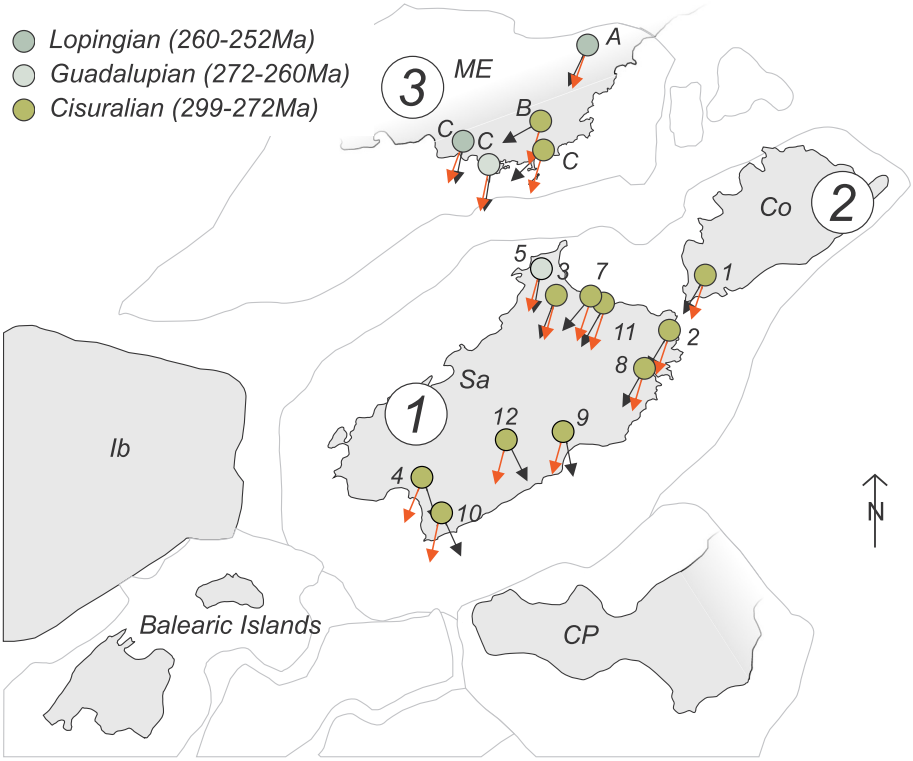

Fig. 11. late Paleozoic to early Mesozoic reconstruction of Maures-Estérel (ME), Corsica (Co), Sardinia (Sa), Iberia (Ib), the Balearic islands and the Calabria-Peloritani terrane (CP). Shown are the expected (red arrows) and observed (solid arrows) paleomagnetic declinations for the Permian. Numbers refers to Table 2. A: Zijderveld (1975), B:Edel (2000) and C: Aubele et al. (2012). All declinations are given in European coordinates using the parameters for the closing of the Ligurian sea (Gattacceca et al., 2007) and the Bay of Biscay (Gong et al., 2008). Stratigraphic age assignments according to Shen and Henderson (2014).

References

Advokaat, E., 2011. New Paleomagnetic Data Show No Mesozoic Rotation of the Corsica-Sardinia Microplate. Master's thesis. Faculty of Geosciences, Utrecht University.

Angiolini, L., Gaetani, M., Muttoni, G., Stephenson, M.H., Zanchi, A., 2007. Tethyan oceanic currents and climate gradients 300 m.y. ago. Geology 35, 1071–1074.

Arthaud, F., Matte, P., 1977. Late Palaeozoic strike-slip faulting in southern Europe and northern Africa: result of a right-lateral shear zone between the Appalachians and the Urals. Geol. Soc. Am. Bull. 88, 1305–1320.

Aubele, K., Bachtadse, V., Muttoni, G., Ronchi, A., 2014. Paleomagnetic data from Late Paleozoic dykes of Sardinia: evidence for block rotations and implications for the intra-Pangea megashear system. Geochem. Geophys. Geosyst. 15, 1684–1697.

Aubele, K., Bachtadse, V., Muttoni, G., Ronchi, A., Durand, M., 2012. A paleomagnetic study of Permian and Triassic rocks from the Toulon-Cuers Basin, SE France: evidence for intra-Pangea block rotations in the Permian. Tectonics 31, TC3015.

Bachtadse, V., 1994. Paläomagnetische Untersuchungen an paläozoischen Gesteinen Afrikas - Implikationen für die Polwanderkurve Gondwanas. Habilitation Thesis. Ludwig-Maximilians University, Munich.

Barca, S., Costamagna, L.G., 2006. Stratigrafia, analisi di facies ed architettura deposizionale della successione permiana di guardia pisano (sulcis, sardegna sw). Boll. Soc. Geol. Ital. 125, 3–19.

Baucon, A., Ronchi, A., Felletti, F., de Carvalho, C.N., 2014. Evolution of crustaceans at the edge of the end-Permian crisis: Ichnonetwork analysis of the fluvial succession of nurra (Permian–Triassic, Sardinia, Italy). Palaeogeogr. Palaeoclimatol. Palaeoecol. 410, 74–103.

Becker, T.P., Thomas, W.A., Samson, S.D., Gehrels, G.E., 2005. Detrital zircon evidence of Laurentian crustal dominance in the lower Pennsylvanian deposits of the Alleghanian clastic wedge in eastern North America. Sediment. Geol. 182, 59–86.

Bourquin, S., 2007. The Permian-Triassic boundary and Early Triassic sedimentation in western European basins: an overview/el límite pérmico-triásico y la sedimentación durante el triásico inferior en las cuencas de europa occidental: una visión general. J. Iber. Geol. 33, 221–236.

Bourquin, S., Bercovici, A., López-Gómez, J., Diez, J.B., Broutin, J., Ronchi, A., Durand, M., Arché, A., Linol, B., Amour, F., 2011. The Permian–Triassic transition and the onset of Mesozoic sedimentation at the northwestern peri-Tethyan domain scale: palaeogeographic maps and geodynamic implications. Palaeogeogr. Palaeoclimatol. Palaeoecol. 299, 265–280.

Broutin, J., Cabanis, B., Chateauneuf, J.J., Deroin, J.P., 1994. Evolution biostratigraphique, magmatique et tectonique du domaine paleotethysien occidental (sw de l9europe); implications paleogeographiques au permien inferieur. Bull. Soc. Geol. Fr. 165, 163–179.

Carmignani, L., Oggiano, G., Funedda, A., Conti, P., Pasci, S., 2016. The geological map of Sardinia (Italy) at 1:250,000 scale. J. Maps 12, 826–835. https://doi.org/10.1080/17445647.2015.1084544.

Cassinis, G., Cortesogno, L., Gaggero, L., Pittau, P., Ronchi, A., Sarria, E., 2000. Late Palaeozoic continental basins of Sardinia. In: Field trip guidebook, Int. Field Conf. on 'The Continental Permian of the Southern Alps and Sardinia (Italy). Regional reports and general correlations', pp. 15–25.

Cassinis, G., Durand, M., Ronchi, A., 2003a. Permian-triassic continental sequences of Northwest Sardinia and south provence: stratigraphic correlations and palaeogeographical implications. Boll. Soc. Geol. Ital. Volume speciale 2, 119–120.

Cassinis, G., Cortesogno, L., Gaggero, L., Ronchi, A., Sarria, E., Serri, R., Calzia, P., 2003b. Reconstruction of igneous, tectonic and sedimentary events in the latest Carboniferous–Early Permian Seui Basin (Sardinia, Italy). Boll. Soc. Geol. It. Volume speciale 2.

Cassinis, G., Perotti, C.R., Ronchi, A., 2012. Permian continental basins in the Southern Alps (Italy) and peri-Mediterranean correlations. Int. J. Earth Sci. 101, 129–157.

Cassinis, G., Ronchi, A., 1997. Upper Carboniferous to Lower Permian continental deposits in Sardinia (Italy). Geodiversitas 19, 217–220.

Cassinis, G., Toutin-Morin, N., Virgili, C., 1995. The Permian of Northern Pangea. Chapter A General Outline of the Permian Continental Basins in Southwestern Europe. vol. 2. Springer, Berlin, Heidelberg, pp. 137–157.

Del Moro, A., Di Pisa, A., Oggiano, G., 1996. Relationships between an Autunian volcano-sedimentary succession and the Tempio massif granites (Northern Sardinia): geochronological and field constraints. Plinius 16.

Domeier, M., van der Voo, R., Torsvik, T.H., 2012. Paleomagnetism and Pangea: the road to reconciliation. Tectonophysics 514-517, 14–43.

Dunlop, D.J., Argyle, K.S., 1997. Thermoremanence, anhysteretic remanence and susceptibility of submicron magnetites: nonlinear field dependence and variation with grain size. J. Geophys. Res. 102, 20199–20210.

Durand, M., 2006. The problem of the transition from the Permian to the Triassic series in southeastern France: comparison with other peritethyan regions. Geol. Soc. Lond. Spec. Publ. 265, 281–296. http://sp.lyellcollection.org/content/265/1/281.full.pdf.

Durand, M., 2008. Permian to triassic continental successions in southern Provence (France); an overview. Boll. Soc. Geol. Ital. 127, 697–716.

Edel, J.B., 2000. Hypothèse d'une ample rotation horaire tardi-varisque du bloc Maures-Estérel-Corse-Sardaigne. Geol. Fr. 1, 3–19.

Edel, J.B., Lacaze, M., Westphal, M., 1981. Palaeomagnetism in the northeastern Central Massif (France): evidence for Carboniferous rotations of the Hercynian orogenic belt. Earth Planet. Sci. Lett. 55, 48–52.

Fischer, J., Schneider, J.W., Ronchi, A., 2010. New hybondontoid shark from the permocarboniferous (Gzhelian–Asselian) of Guardia Pisano (Sardinia, Italy). Acta Palaeontol. Pol. 55, 241–264.

Fisher, R., 1953. Dispersion on a sphere. Proc. R. Soc. Lond. A Math. Phys. Eng. Sci. 217, 295–305. http://rspa.royalsocietypublishing.org/content/217/1130/295.full.pdf.

Fluteau, F., Besse, J., Broutin, J., Berthelin, M., 2001. Extension of Cathaysian flora during the Permian climatic and paleogeographic constraints. Earth Planet. Sci. Lett. 193, 603–616.

Gaggero, L., Gretter, N., Langone, A., Ronchi, A., 2017. U–Pb geochronology and geochemistry of late palaeozoic volcanism in Sardinia (southern Variscides). Geosci. Front. 8, 1263–1284.

Gallo, L.C., Tomezzoli, R.N., Cristallini, E.O., 2017. A pure dipole analysis of the Gondwana apparent polar wander path: paleogeographic implications in the evolution of Pangea. Geochem. Geophys. Geosyst. 18, 1499–1519.

Galtier, J., Ronchi, A., Broutin, J., 2011. Early Permian silicified floras from the Perdasdefogu basin (SE Sardinia): comparison and bio-chronostratigraphic correlation with the floras of the Autun basin (Massif Central, France). Geodiversitas 33, 43–69.

Gasperi, G., Gelmini, R., 1980. Ricerche sul verrucano. 4. il verrucano della nurra (sardegna nord-occidentale). Mem. Soc. Geol. Ital. 20, 215–231.

Gattacceca, J., Deino, A., Rizzo, R., Jones, D., Henry, B., Beaudoin, B., Vadeboin, F., 2007. Miocene rotation of Sardinia: new paleomagnetic and geochronological constraints and geodynamic implications. Earth Planet. Sci. Lett. 258, 359–377.

Gong, Z., Langereis, C.G., Mullender, T.A.T., 2008. The rotation of Iberia during the Aptian and the opening of the Bay of Biscay. Earth Planet. Sci. Lett. 273, 80–93.

Gretter, N., Ronchi, A., López-Gómez, J., Arche, A., De la Horra, R., Barrenechea, J., Lago San José, M., 2015. The Late Palaeozoic-Early Mesozoic from the Catalan pyrenees (Spain): 60 Myr of environmental evolution in the frame of the western peri-Tethyan palaeogeography. Earth Sci. Rev. 150, 679–708.

Irving, E., 1967. Paleomagnetic evidence for shear along the Tethys. pp. 59–76.

Irving, E., 1977. Drift of the major continental blocks since the Devonian. Nature 270, 304–309.

Kirscher, U., Aubele, K., Muttoni, G., Ronchi, A., Bachtadse, V., 2011. Paleomagnetism of Jurassic carbonate rocks from Sardinia: no indication of post-jurassic internal block rotations. J. Geophys. Res. Solid Earth 116, B12107.

Kirschvink, J.L., 1980. The least-squares line and plane and the analysis of palaeomagnetic data. Geophys. J. R. Astron. Soc. 62, 699–718.

Krása, D., Fabian, K., 2007. Rock Magnetism, Hysteresis Measurements. Springer, Dordrecht.

Leonhardt, R., Soffel, H.C., 2006. The growth, collapse and quiescence of teno volcano, tenerife; new constraints from paleomagnetic data. Geol. Rundsch. Int. J. Earth Sci. (1999) 95, 1053–1064.

Manspeizer, W., 1988. Chapter 3 - Triassic–Jurassic rifting and opening of the Atlantic: an overview. In: Manspeizer, W. (Ed.), Triassic-Jurassic Rifting. Developments in Geotectonics. vol. 22. Elsevier, pp. 41–79.

McFadden, P.L., Reid, A.B., 1982. Analysis of palaeomagnetic inclination data. Geophys. J. R. Astron. Soc. 69, 307–319. https://doi.org/10.1111/j.1365-246X.1982.tb04950.x.

McKenzie, D., Jackson, J., 1983. The relationship between strain rates, crustal thickening, palaeomagnetism, finite strain and fault movements within a deforming zone. Earth Planet. Sci. Lett. 65, 182–202.

Morel, P., Irving, E., 1978. Tentative paleocontinental maps for the early phanerozoic and proterozoic. J. Geol. 86, 535–561. https://doi.org/10.1086/649724.

Morel, P., Irving, E., 1981. Paleomagnetism and the evolution of Pangea. J. Geophys. Res. Solid Earth 86, 1858–1872.

Morel, P., Irving, E., Daaly, L., Moussine-Pouchkine, A., 1981. Paleomagnetic results from Permian rocks of the northern Saharan craton and motions of the Moroccan Meseta and Pangea. Earth Planet. Sci. Lett. 55, 65–74.

Moskowitz, B., 1981. Methods for estimating curie temperatures of titanomaghemites from experimental J_s-T data. Earth Planet. Sci. Lett. 53, 84–88.

Muttoni, G., Gaetani, M., Kent, D.V., Sciunnach, D., Angiolini, L., Berra, F., Garzanti, E., Mattei, M., Zanchi, A., 2009. Opening of the neo-Tethys ocean and the Pangea b to Pangea a transformation during the Permian. GeoArabia (Manama) 14, 17–48.

Muttoni, G., Kent, D., Garzanti, E., Brack, P., Abrahamsen, N., Gaetani, M., 2003. Early Permian Pangea 'B' to Late Permian Pangea 'A'. Earth Planet. Sci. Lett. 215, 379–394.

Nicholson, C., Seeber, L., Williams, P., Sykes, L.R., 1986. Seismicity and fault kinematics through the eastern transverse ranges, California: block rotation, strike-slip faulting and low-angle thrusts. J. Geophys. Res. Solid Earth 91, 4891–4908. https://doi.org/10.1029/JB091iB05p04891.

Pecorini, G., 1974. Nuove osservazioni sul permo-trias di escalaplano (sardegna sud-orientale. Boll. Soc. Geol. Ital. 93, 991–999.

Pittau, P., Barca, S., Cocherie, A., Rio, M.D., Fanning, M., Rossi, P., 2002. Le bassin permien de guardia pisano (sud-ouest de la sardaigne, italie): palynostratigraphie, paléophytogéographie, corrélations et âge radiométrique des produits volcaniques associés. Geobios 35, 561–580.

Ronchi, A., Broutin, J., Diez, J., Freytet, P., Galtier, J., Lethiers, F., 1998. New palaeontological discoveries in some Early Permian sequences of Sardinia. Biostratigraphic and palaeogeographic implications. C. R. Acad. Sci. Ser. IIA - Earth Planet. Sci. 327, 713–719.

Ronchi, A., Sacchi, E., Romano, M., Nicosia, U., 2011. A huge caseid pelycosaur from north-western Sardinia and its bearing on European Permian stratigraphy and palaeobiogeography. Acta Palaeontol. Pol. 56, 723–738.

Ronchi, A., Sarria, E., Broutin, J., 2008. The "Autuniano Sardo": basic features for a correlation through the Western Mediterranean and Paleoeurope. Boll. Soc. Geol. Ital. 127, 655–681.

Shen, S.Z., Henderson, C.M., 2014. Progress of the Permian timescale. In: Rocha, R., Pais, J., Kullberg, J.C., Finney, S. (Eds.), STRATI 2013. Springer International Publishing, Cham, pp. 447–451.

Sinisi, R., Mongelli, G., Mameli, P., Oggiano, G., 2014. Did the Variscan relief influence the Permian climate of mesoeurope? Insights from geochemical and mineralogical proxies from Sardinia (Italy). Palaeogeogr. Palaeoclimatol. Palaeoecol. 396.

Tauxe, L., 2010. Essentials of Paleomagnetism. University of California Press, Berkeley.
Tauxe, L., Kent, D.V., 2004. A Simplified Statistical Model for the Geomagnetic Field and the Detection of Shallow Bias in Paleomagnetic Inclinations: Was the Ancient Magnetic Field Dipolar? American Geophysical Union, pp. 101–115. https://doi.org/10.1029/145GM08.
Torsvik, T.H., der Voo, R.V., Preeden, U., Niocaill, C.M., Steinberger, B., Doubrovine, P.V., van Hinsbergen, D.J., Domeier, M., Gaina, C., Tohver, E., Meert, J.G., McCausland, P.J., Cocks, L.R.M., 2012. Phanerozoic polar wander, palaeogeography and dynamics. Earth Sci. Rev. 114, 325–368.
Traversa, G., 1979. Permian volcanism in Sardinia. IGCP Project, Newsletter. 1. pp. 127–140.
Vai, G., 2003. Development of the palaeogeography of Pangaea from Late Carboniferous to Early Permian. Palaeogeogr. Palaeoclimatol. Palaeoecol. 196, 125–155.
Van Hilten, D., 1964. Evaluation of some geotectonic hypotheses by paleomagnetism. Tectonophysics 1, 3–71.
Vigliotti, L., Alvarez, W., McWilliams, M., 1990. No relative rotation detected between corsica and Sardinia. Earth Planet. Sci. Lett. 98, 313–318.
Virgili, C., Cassinis, G., Broutin, J., 2006. Permian to triassic sequences from selected continental areas of southwestern Europe. Geol. Soc. Lond. Spec. Publ. 265, 231–259. http://sp.lyellcollection.org/content/265/1/231.full.pdf.
Werneburg, R., Ronchi, A., Schneider, J.W., 2007. The Early Permian branchiosaurids (amphibia) of Sardinia (Italy): systematic palaeontology, palaeoecology, biostratigraphy and palaeobiogeographic problems. Palaeogeogr. Palaeoclimatol. Palaeoecol. 252, 383–404.
Westphal, M., Orsini, J., Vellutini, P., 1976. Le microcontinent corso-sarde, sa position initiale: Donnees paléomagnétiques et raccords géologiques. Tectonophysics 30, 141–157.
Zijderveld, J.A.C., 1967. Demagnetization of rocks: analysis of results. In: Collinson, D.W., Creer, K.M., Runcorn, S.K. (Eds.), Methods in Paleomagnetism. Elsevier, Amsterdam, pp. 254–286.
Zijderveld, J., 1975. Paleomagnetism of the Esterel Rocks. PhD thesis. Utrecht University.
Zijderveld, J.D.A., De Jong, K.A., Van der Voo, R., 1970. Rotation of Sardinia: palaeomagnetic evidence from Permian rocks. Nature 226, 993–994.